American Mineralogist, Volume 83, pages 444–450, 1998

Sound velocities of polycrystalline $MgSiO_3$-orthopyroxene to 10 GPa at room temperature

LUCY M. FLESCH,[1,*] BAOSHENG LI,[2] and ROBERT C. LIEBERMANN[1]

[1]Center for High Pressure Research and Department of Geosciences, State University of New York at Stony Brook, Stony Brook, New York 11794-2100, U.S.A.
[2]Center for High Pressure Research and Mineral Physics Institute, State University of New York at Stony Brook, Stony Brook, New York 11794-2100, U.S.A.

ABSTRACT

A polycrystalline sample of $MgSiO_3$-orthopyroxene was hot pressed at a pressure of 4 GPa and temperature of 975 °C in a multi-anvil apparatus. The recovered specimen has a bulk density within 1% of the X-ray density and compressional and shear wave velocities within 1% of the Hashin-Shtrikman averages of the isotropic velocities calculated from the single-crystal elastic moduli. Compressional and shear wave travel times were measured at pressures up to 10 GPa at room temperature using the phase comparison method of ultrasonic interferometry in a 1000 ton uniaxial split-cylinder apparatus (USCA-1000). The velocities and elastic moduli monotonically increase with pressure; discontinuous behavior is not observed. Both the compressional velocity and bulk modulus, however, exhibit pronounced non-linear dependence on pressure. Fitting a fourth-order Eulerian finite-strain equation of state yield values of the bulk modulus and its first and second pressure derivatives, K_0 = 104(2) GPa, K_0' = 10.9(5), and K_0'' = −1.6(2) GPa^{-1}. In contrast, the shear velocity and modulus are linear with pressure, yielding values of G_0 = 74.9(1.5) GPa and G_0' = 1.6(1), when fit to a third-order finite-strain equation of state. A *P-V* trajectory calculated from these continuous measurements of *K* vs. *P* to 8 GPa is in agreement with extant static compression data for this material, without requiring a discontinuous change in *K* at 4 GPa. The velocities of $MgSiO_3$-orthopyroxene increase more rapidly with pressure than those for Mg_2SiO_4-olivine (especially for P-waves), such that these two mineral phases are virtually indistinguishable in their velocities at 200 km depth, unless the velocity-temperature dependence of the two phases is dramatically different.

INTRODUCTION

Orthopyroxene is the second most abundant phase in the Earth's upper mantle and its elastic properties are important in interpreting seismic velocity models. Until recently, experimental difficulties have limited the available data for sound velocities in orthopyroxenes (opx) to pressures less than 4 GPa at room temperature.

The adiabatic bulk modulus of orthoenstatite at ambient pressure, K_0 = 108 GPa, can be calculated from the single-crystal elastic moduli measured by Brillouin spectroscopy (Weidner et al. 1978). Frisillo and Barsch (1972) used ultrasonic pulse superposition to determine the elastic properties of a natural $(Mg_{0.8}Fe_{0.2})SiO_3$-opx single crystal to 1 GPa and measured an unusually high value of the pressure derivative of the bulk modulus, K_0' = 9.6. This is significantly higher than K_0' observed for other mantle minerals, typically between four and six. Ito et al. (1977), in an ultrasonic study from 2 to 4 GPa on a polycrystal of $MgSiO_3$, also measured a high value of K_0' = 10.7. In a later ultrasonic study of natural $(Mg_{0.8}Fe_{0.2})SiO_3$-opx single crystals, Webb and Jackson (1993) measured a high initial value of K_0' = 10.8, but observed a significant second pressure derivative, K_0'' = −1.6 GPa^{-1}; consequently, d*K*/d*P* decreases from 10.8 at zero pressure to ~5 or 6 at 3 GPa. This unusual behavior of the elastic moduli of orthopyroxene casts uncertainty on any attempts to extrapolate the sound velocities to higher pressures.

In a static compression study of $MgSiO_3$-opx to 8 GPa (Hugh-Jones and Angel 1994), a change in slope was observed in the volume vs. pressure plot around 4 GPa; although no change in crystal symmetry was observed. Hugh-Jones and Angel (1994) fit the *P-V* data above and below 4 GPa with different equations of state and concluded that the mechanism by which the orthopyroxene crystals accommodate the decrease in volume under pressure changes near this critical pressure. A second-order discontinuity in the *P-V* trajectory as observed for $MgSiO_3$-opx by Hugh-Jones and Angel (1994) should be manifest as a first-order discontinuity in the compressibility (or the bulk modulus, the incompressibility), which is the slope of the *P-V* curve at any pressure (as also shown in Fig. 4 of Chai et al. 1998).

Because it is now possible in our laboratory and others to measure the acoustic velocities of single crystal or po-

* E-mail: flesch@sbmp04.ess.sunysb.edu

0003–004X/98/0506–0444$05.00

TABLE 1. The pressure and temperature path for the hot-pressed polycrystalline sample and its bench top measurements

	Hot pressing conditions								
Sample	P (GPa)	T (°C)	Experiment duration (min)	Annealing T (°C)	ρ (g/cm³)	V_p (km/sec)	V_s (km/sec)	K_s (GPa)	G (GPa)
K292	4	975	45	600	3.18	8.03	4.82	107	74.5
Weidner et al. (1978) (Hashin-Shtrikman averages)					3.204*	8.07	4.86	108	75.7

* Sasaki et al. (1982).

lycrystalline samples to 12 GPa at room temperature using ultrasonic techniques in a multi-anvil apparatus (Li et al. 1996a, 1997; Knoche et al. 1995, 1996), we can directly measure the bulk modulus and its pressure dependence in orthopyroxene to mantle pressures. This paper presents new elasticity data for polycrystalline $MgSiO_3$-orthopyroxene to 10 GPa at room temperature using in situ ultrasonic interferometry.

EXPERIMENTAL METHODS

A polycrystalline sample of $MgSiO_3$-opx was hot pressed in a 1000 ton uniaxial split-cylinder apparatus (USCA-1000, Li et al. 1996a) using the techniques developed by Gwanmesia and Liebermann (1992). We used a standard 14/8 mm graphite box furnace assembly [shown in Fig. 2 of Gwanmesia and Liebermann (1992)] except that the Ta Plates were replaced with graphite disks. Pieces of a single crystal grown by J. Ito (1975) and given to us by Y. Zhao were crushed into a fine powder and used as a starting material; these crystals were from the same batch as those used by Weidner et al. (1978) in their Brillouin measurements. Pressure, temperature, and experiment duration at peak conditions are shown in Table 1 for the hot-pressed sample. The sample was decompressed using path 3 of Gwanmesia and Liebermann (1992) and annealed at 600 °C during decompression. An X-ray powder diffraction pattern taken from the end of the cylindrical specimen K292 (Fig. 1) confirms the orthopyroxene structure. The density of the polycrystal, determined using the Archimedes method and CCl_4 liquid, is within 1% of the theoretical X-ray density of Sasaki et al. (1982), with an average grain size ≤10 μm determined by SEM. The bench top velocities (Table 1) are within 1% of the isotropic velocities calculated using the Hashin-Shtrikman averaging schemes from the single-crystal elastic moduli of Weidner et al. (1978). After polishing to a 1 μm finish, the sample was 2.412(3) mm long and 3 mm in diameter, determined using a digital micrometer.

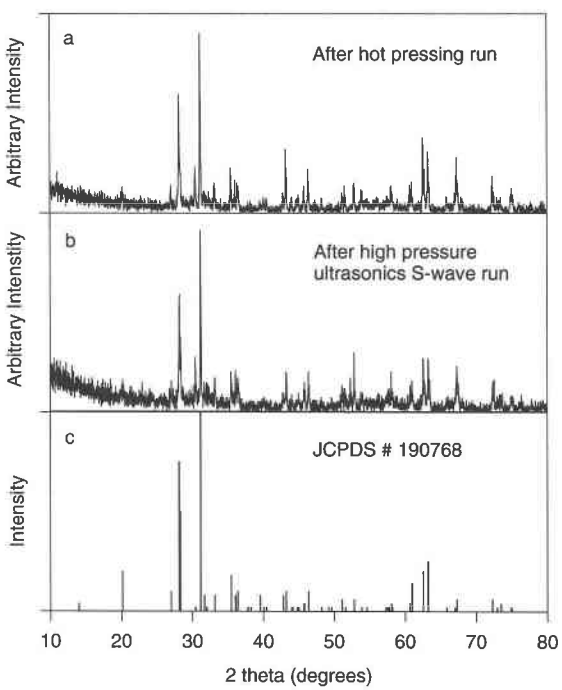

FIGURE 1. X-ray powder diffraction patterns for $MgSiO_3$-opx: (**a**) sample K292 after the hot-pressing experiment and before the high-pressure ultrasonic experiments; (**b**) sample K292 after the high-pressure S-wave ultrasonic experiment; (**c**) the standard JCPDS card entry no. 190768. No structural change was observed in the sample after the high-pressure ultrasonic experiment.

Compressional and shear wave travel times were measured as a function of pressure to 10 GPa in the USCA-1000 multi anvil apparatus using the techniques described by Li et al. (1996a) and the cell assembly of Figure 2. The sample was surrounded by lead to create a pseudo-hydrostatic pressure environment with a pressure gradient less than 0.25 GPa/mm along the specimen axis (Li et al. 1996a). Resistance changes due to phase transitions in Bi (at 2.55 and 7.7 GPa), placed inside the cell during the S-wave experiment, and in ZnTe (at 9.6 GPa) for the P-wave experiment, were used as markers to create a hybrid pressure scale for the sample. As shown by Li et al. (1996a) the reproducibility of the cell pressure is within 1% for a given oil pressure for the same sample.

A 40 MHz $LiNbO_3$ transducer was bonded to a tungsten carbide cube, which was used as an acoustic buffer rod. The phase comparison method of ultrasonic interferometry (e.g., Niesler and Jackson 1989; Rigden et al. 1992) was used to determine the travel time through the polycrystalline sample. The echo pattern for S-waves at 10 GPa is shown in Figure 3, and the interference pattern of the buffer rod and the first sample echo from this echo pattern is shown in Figure 4. At 10 GPa we still have a high-amplitude acoustic signal and sharp minima in the

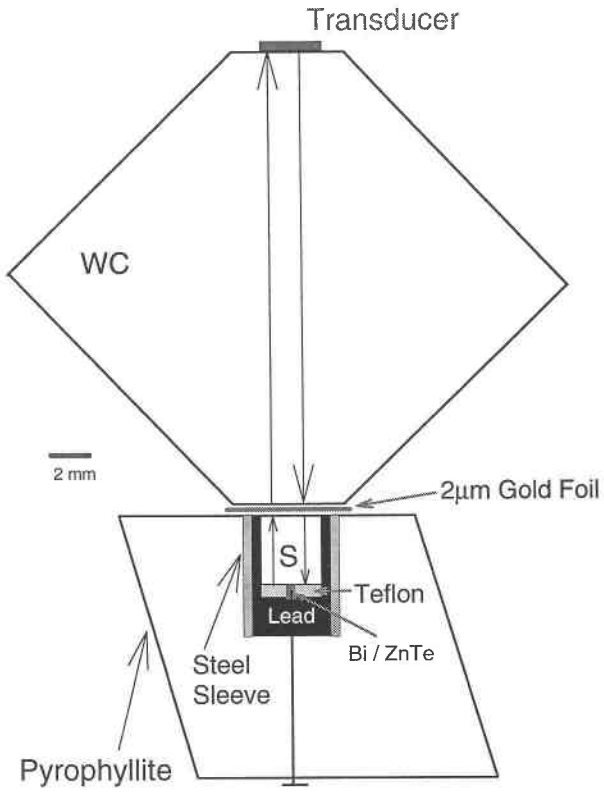

FIGURE 2. A cross section of acoustic cell assembly used in measuring sound velocities as a function of pressure (see additional details in Li et al. 1997).

interference pattern, which demonstrate the mechanical integrity of our specimen even at this pressure. Travel times at each pressure are shown in Figure 5 for the P-wave and S-wave experiments on K292. For both P- and S-waves, the dispersion curves reach stable travel time values at high frequency that allow us to determine the velocities at all pressures with a precision of 0.5%. It is not known what causes the small offset in travel times for S-waves near the resonance frequency of the $LiNbO_3$ transducers (which has also been observed in experiments on other materials), but it is within the stated precision of our velocity data.

RESULTS AND DISCUSSION

An S-wave experiment was performed on sample K292 and upon recovery of the sample, no bench top signal could be observed. Sample K292 was then re-run in a P-wave experiment and when it was pressurized to ~1 GPa the acoustic echoes reappeared and P-wave data were obtained to 10 GPa. Length corrections for the sample were calculated using the method of Cook (1957), bond corrections were made (Davies and O'Connell 1977; Jackson et al. 1981; Niesler and Jackson 1989), and the velocities were calculated. Figure 6 shows the velocity profiles for sample K292 from the two velocity experiments. The lack of signal after the high-pressure ultrasonic experiments is

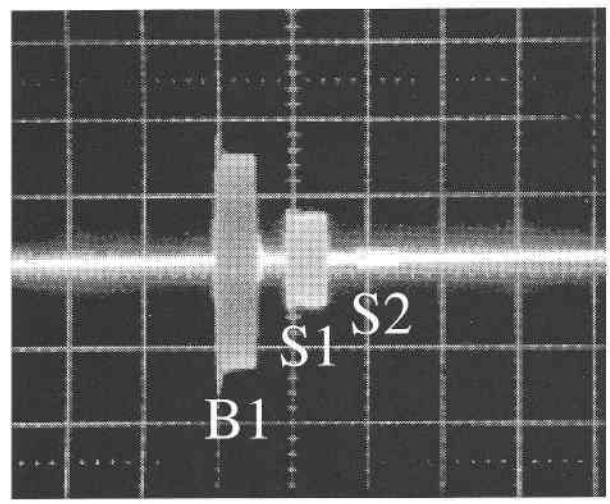

FIGURE 3. Acoustic signals from the S-wave experiment on polycrystalline $MgSiO_3$-opx, sample K292, at ~10 GPa. The first echo represents a reflection off the buffer rod (B1), the second and third (S1, S2) are reflections from within the sample.

interpreted as being caused by micro-cracks that developed during a slow decompression at room temperature and that closed upon recompression. The density and length of the recovered sample agree, within the experimental uncertainty, with its initial values. The velocities measured from the P-wave experiment on the re-run sample agree within 0.5% with velocities from a fresh $MgSiO_3$-opx polycrystal experiment in the same assembly (Flesch 1997).

Changes in the Raman spectra of natural orthopyrox-

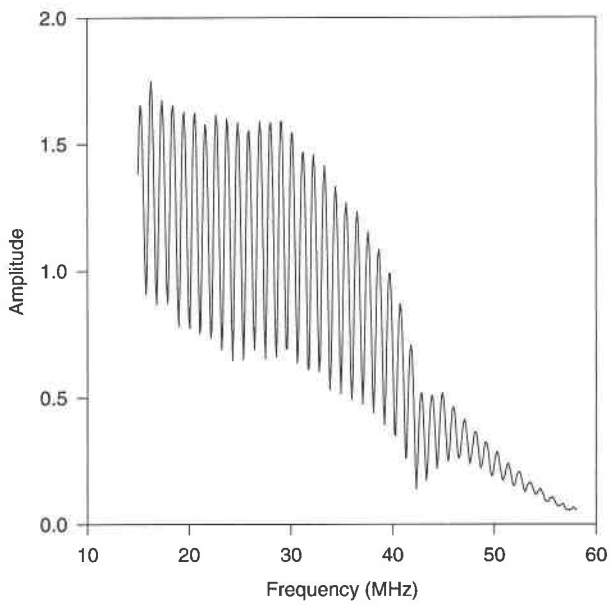

FIGURE 4. Interference pattern at ~10 GPa between the buffer rod echo (B1) and the first sample echo (S1) from the S-wave experiment of $MgSiO_3$-opx sample K292.

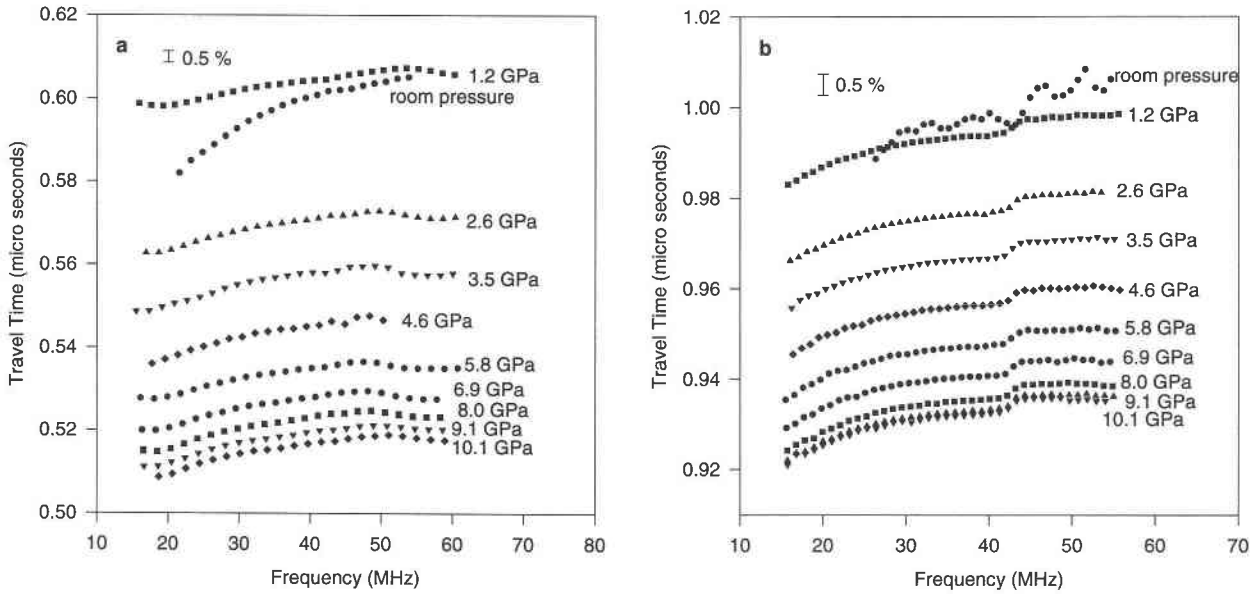

FIGURE 5. Travel time dispersion curves at each pressure for the (**a**) P-wave experiment and (**b**) S-wave experiment on $MgSiO_3$-opx sample K292. Vertical bars represent the 0.5% precision of the travel time measurement (see also Table 2).

enes around 10 GPa at room temperature were interpreted by Hugh-Jones et al. (1997) as a phase transformation to the high-clinopyroxene structure, which back transforms to the low-clinopyroxene structure upon decompression (see also Pacalo and Gasparik 1990). However, an X-ray powder diffraction pattern of our sample K292 after the high-pressure ultrasonic experiment (Fig. 1) suggests that the structure remained orthopyroxene throughout the experiment. Orthopyroxene is metastable throughout the pressure range of this study.

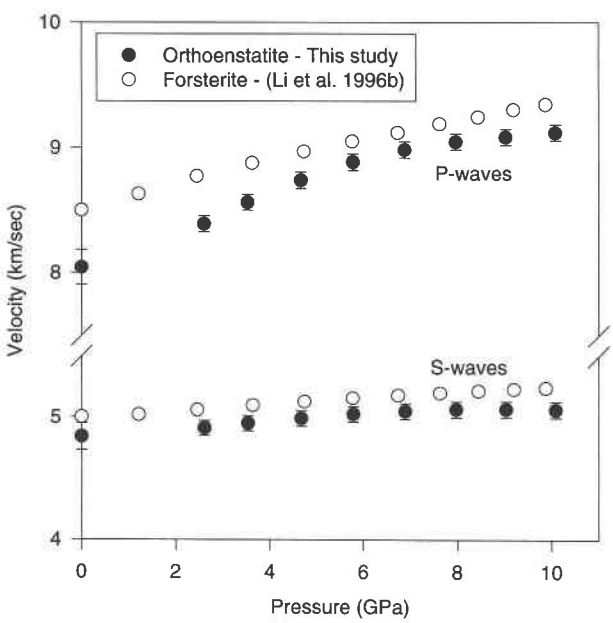

FIGURE 6. Comparison of the compressional and shear wave velocities for polycrystalline $MgSiO_3$-opx, K292 (closed circles) from this study and Mg_2SiO_4-olivine (forsterite) from Li et al. (1996b). Error bars represent 1% precision of the velocity measurements of K292 at high pressure (see also Table 2).

Table 2 gives the travel times, sample length, and calculated velocities and bulk and shear moduli for the P- and S-wave experiments for sample K292. The travel times at 1 bar were measured outside the press by bonding the sample to a glass buffer rod with a Dow-Corning silicone grease (V-9) bond; with appropriate bond corrections (Davies and O'Connell 1977; Jackson et al. 1981; Niesler and Jackson 1989), the 1 bar velocities are well determined. The travel times at 1 bar exhibit a greater dispersion than those at higher pressures due to the difference in bonding material; however, the data at 1 bar are well determined and are included in the data set because of the agreement with the single-crystal data of Weidner et al. (1978). Because the cell assembly is compressed slowly from 1 bar to 2 GPa, the mechanical contact gradually improves between the tungsten carbide buffer rod and the sample by means of a gold foil bond. In our analysis below, the data at 1.2 GPa are not included because of the incomplete contact (see Figs. 5a and 5b).

The moduli from sample K292 were calculated and fit to both third- and fourth-order Eulerian finite-strain equations of state (e.g., Davies and Dziewonski 1975, p. 337) as shown in Figure 7. There is considerable curvature in the bulk modulus vs. pressure data that cannot be satisfied with a simple third-order fit; a significant second pressure derivative is required to satisfy the bulk moduli data. Performing an F_x test of an additional term, (Bevington and Robinson 1996, page 209) yields a value of 7.16 for the

TABLE 2. Elastic properties of polycrystalline $MgSiO_3$-opx (sample K292)

Pressure (GPa)	$2t_p$ (μsec)	$2t_s$ (μsec)	2 length (mm)	V_p (km/sec)	V_s (km/sec)	ρ (g/cm³)	K_s (GPa)	G (GPa)
0.00	0.600(3)	1.00(1)	4.824(6)	8.03(14)	4.82(8)	3.18(3)	107(5)	75(3)
2.62(50)	0.571(3)	0.978(5)	4.787(5)	8.39(6)	4.91(4)	3.25(3)	125(3)	78(2)
3.54(50)	0.558(3)	0.968(5)	4.776(6)	8.56(6)	4.95(4)	3.28(3)	133(3)	80(2)
4.67(50)	0.545(3)	0.958(5)	4.762(6)	8.74(6)	4.99(4)	3.31(3)	143(3)	82(2)
5.79(50)	0.535(3)	0.949(5)	4.750(6)	8.89(6)	5.02(4)	3.33(3)	151(3)	84(2)
6.89(50)	0.528(3)	0.942(5)	4.739(7)	8.98(6)	5.05(4)	3.36(3)	157(3)	85(2)
7.97(50)	0.523(3)	0.937(5)	4.728(7)	9.05(6)	5.06(4)	3.38(3)	161(3)	87(2)
9.04(50)	0.520(3)	0.935(5)	4.718(7)	9.09(6)	5.06(4)	3.40(3)	164(3)	87(2)
10.1(5)	0.517(3)	0.934(5)	4.708(7)	9.12(6)	5.06(4)	3.42(3)	168(3)	88(2)

bulk moduli data, which allows us to say within a 95% confidence limit that the additional fourth-order term has improved the fit without overfitting the data. The shear modulus can be described by a third-order finite-strain equation; a fourth-order finite-strain equation yields virtually the same G_0 and G_0' as the third-order fit and a second pressure derivative of -0.12 GPa^{-1}; again performing the F_x test of an additional term for the shear moduli, yields a value of 1.5×10^{-7} showing that the fourth-order term is not needed and only introduces random errors to the fit. Table 3 gives the values of the bulk and shear moduli and their first and second pressure derivatives for both equations based on third- and fourth-order finite strain and linear and quadratic formulations.

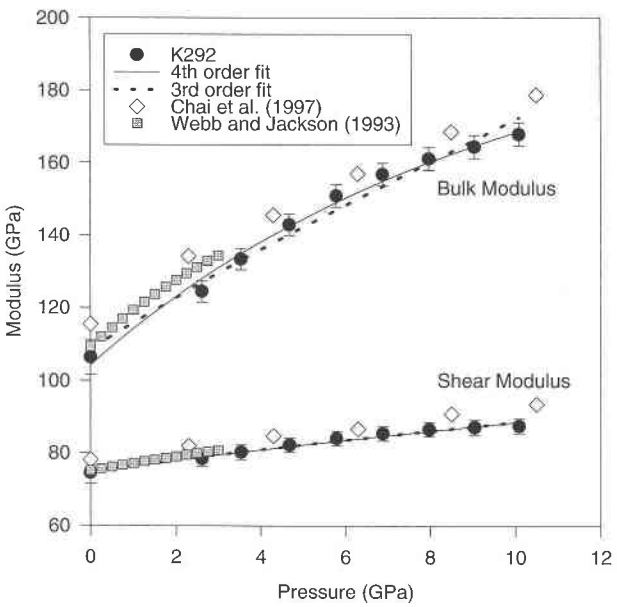

FIGURE 7. Calculated elastic moduli for polycrystalline $MgSiO_3$-opx vs. pressure for sample K292 (closed circles). Third- and fourth-order finite-strain fits to K292 are shown as dotted and solid lines, respectively (see also Table 3). The calculated moduli for K292 are also compared with orthopyroxenes of different compositions. The shaded squares represent ultrasonic data from Webb and Jackson (1993) with composition $(Mg_{0.8},Fe_{0.2})SiO_3$, 1 wt% of Al_2O_3, and 0.2 wt% each of MnO and CaO; the open diamonds represent the impulsive-simulated scattering data from Chai et al. (1997) with composition $(Mg_{0.9},Fe_{0.1})SiO_3$, 1 wt% CaO, and 5 wt% Al_2O_3.

The form of the equations used to fit the data will influence the elastic parameters extracted particularly for samples exhibiting non-linear behavior of elastic constants with pressure. For example, although both the fourth-order finite strain and the quadratic polynomial equations fit our bulk modulus data equally well over the pressure range of our experiments, the values of K_0' differ by 14% and those of K_0'' by a factor of 2 (Table 3). Similar comments apply to the bulk modulus data for the Kilbourne Hole opx of Chai et al. (1998). Therefore, elastic moduli from different studies must be compared using the same equations of state. In the same vein, extrapolations of such data to higher pressure should be made using the same equations as those used in fitting the data; for example, extrapolations made using a quadratic polynomial and our finite-strain values yield a bulk modulus that reaches a maximum at ~8 GPa and then begins to decrease as a function of increasing pressure.

The bulk moduli is a continuous function of pressure over the entire experimental range to 10 GPa (Fig. 7). We observe no first-order discontinuity in the K-P behavior, as would be suggested by the change in slope in the P-V trajectory observed by Hugh-Jones and Angel (1994) at 4 GPa (which imply a decrease of K by 10 GPa at that pressure). The large value of K_0'' observed in our study, however, may reflect a gradual change in the compression mechanism over the larger pressure range we studied. Initially the compressible M2-O bonds allow kinking of the SiO_4 tetrahedral chain, which yield an anomalous high value of K_0' (Webb and Jackson 1990). As compression continues, the individual tetrahedra begin to compress (Hugh-Jones and Angel 1994), which lowers the value of K_0' requiring a significant negative K_0''. This change in compression mechanism is reflected in the curvature of our data, but the continuous increase in moduli with pressure suggests that the change is gradual.

The bulk modulus and pressure derivatives obtained in this study from the fourth-order finite-strain fit (Table 3), generated a P-V trajectory, which compares well with the P-V data of Hugh-Jones and Angel (1994) and Zhao et al. (1995) from single crystals of $MgSiO_3$-opx (Fig. 8). Thus, a single equation of state can describe the compression of $MgSiO_3$-opx to 8 GPa at room temperature,

TABLE 3. Elastic moduli and their pressure derivatives for orthopyroxenes

K_0 (GPa)	K_0'	K_0'' (GPa^{-1})	G_0 (GPa)	G_0'	G_0'' (GPa^{-1})		
109(2)	7.0(4)	(−0.17)	74.9(1.5)	1.6(1)		ultrasonic	K292* third-order finite strain
104(2)	10.9(5)	−1.6(2)	74.8(1.5)	1.4(1)	−0.12(1)	ultrasonic	K292* fourth-order finite strain
110(2)	6.2(3)		75.3(1.5)	1.4(1)		ultrasonic	K292* linear
105(2)	9.5(5)	−0.64(6)	74.1(1.5)	2.0(1)	−0.14(1)	ultrasonic	K292* quadratic
109.4(5)	10.8(8)	−1.6(2)	75.2(4)	2.06(7)	−0.12(0)	ultrasonic	Webb and Jackson (1993)‡ quadratic
115.5(5)	7.82	−0.35	78.1(4)	1.45		ISS	Chai et al. (1997)†-polynomial
116	8.3	−0.66	77.9	1.6		ISS	finite strain fit to data of Chai et al. (1997)†

Notes: Third- and fourth-order Eulerian finite strain (Davies and Dziewonski 1975, p 337). Linear: $K = K_0 + K_0'P$. Quadratic: $K = K_0 + K_0'P + \frac{1}{2}K_0''P^2$. K_0 = Bulk Modulus at 1 bar; $K_0' = (dK/dP)_T$; $K_0'' = (d^2K/dP^2)_T$. G_0 = Shear Modulus at 1 bar; $G_0' = (dG/dP)_T$; $G_0'' = (d^2G/dP^2)_T$. ISS = impulse-stimulate scattering.

* $MgSiO_3$.

‡ $(Mg_{0.8}Fe_{0.2})SiO_3$, with 1 wt% of Al_2O_3, and 0.2 wt% each of MnO and CaO.

† $(Mg_{0.9}Fe_{0.1})SiO_3$, also containing 1 wt% CaO and 5 wt% Al_2O_3.

without invoking a discontinuous change in K at 4 GPa. Similar conclusions were inferred by Chai et al. (1997); however, their calculated P-V trajectory lies above the measured data over the entire pressure range as a consequence of a higher K_0 and a K_0' value, which is 59% smaller than ours as a result of the different composition of their specimen.

Our new bulk and shear moduli data for $MgSiO_3$-opx to 10 GPa lie on the trend of Webb and Jackson (1993) ultrasonic data from lower pressures (Fig. 7), although due to differences in pressure ranges of the two studies, the moduli and derivatives from the quadratic fits cannot be compared. In contrast, elasticity data for the Kilbourne Hole crystal of Chai et al. (1997) to 12 GPa (Table 3, Fig. 7) exhibit less curvature with pressure than the orthoenstatite data. This is consistent with the data and interpretation of Hugh-Jones et al. (1997), which suggest that substitution of the larger Ca^{2+} for Mg^{2+} in the M2 site shortens and stiffens the M2-O bonds, resulting in a lower K_0' and less negative K_0''. The Kilbourne Hole crystals also contain ~5 wt% Al in the tetrahedral site, which may effect the compressibility by stiffening the tetrahedral chain (Chai et al. 1997).

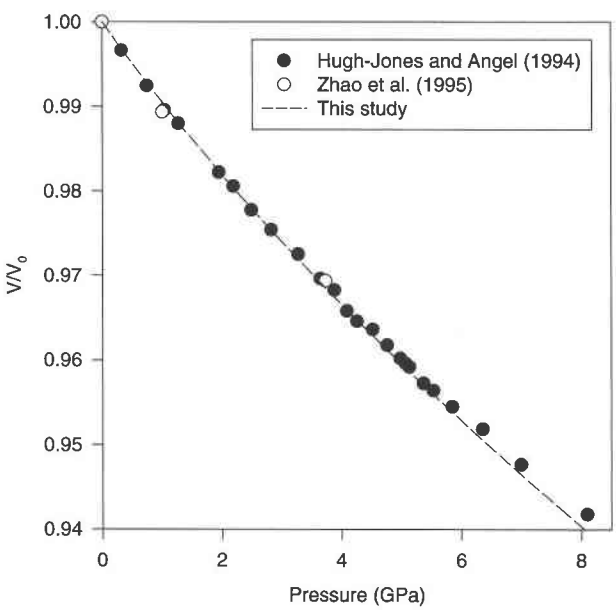

FIGURE 8. P-V data measured in static compression experiments by Hugh-Jones and Angel (1994) (closed circles) and Zhao et al. (1995) (open circles). The dashed line is a fourth-order equation of state generated using the K_{T0}, ($\alpha = 24.1 \times 10^{-6}\ K^{-1}$, $\gamma = 9.53$), and K_0', and K_0'' measured in this study (Table 3).

Finally, we compare our new velocity data for orthoenstatite ($MgSiO_3$-opx) with those for forsterite (Mg_2SiO_4-olivine) from Li et al. (1996b). At ambient conditions, the P-wave velocity of orthopyroxene is 6% lower than that of olivine (Fig. 6). As a consequence of the difference in their K-P behavior, however, the velocities of these two major mineral components of the upper mantle converge rapidly and are nearly equal at 6.5 GPa, the room-temperature metastable boundary between the orthopyroxene and high-clinopyroxene phases (Gasparik 1990). Thus, on the basis of P-wave velocities, these two phases are virtually indistinguishable at 200 km depth in the Earth, unless the velocity-temperature dependence of the two phases is dramatically different.

ACKNOWLEDGMENTS

We thank Yusheng Zhao and Jun Liu for giving us the orthoenstatite crystals; Carey Koleda, Herb Schay, and Ed Vorisek for fabricating tools and cell parts for the high-pressure experiments; Ben Vitale for computer software to operate the press and Gabriel Gwanmesia for hot pressing advice and assistance. We have benefited from conversations with Ross Angel, Stephen Finch, and Ian Jackson. We thank M. Chai, J.M. Brown, and L. Slutsky for the preprint of their paper, and Sharon Webb and Ian Jackson for providing us with their original velocity data. We also thank Ruth Knoche, Robert Luth, and an anonymous reviewer for their time and constructive criticism that improved the manuscript. These high-pressure experiments were conducted in the Stony Brook High Pressure Laboratory, which is jointly supported by the State University of New York at Stony brook and the NSF Science and Technology Center for High Pressure Research (EAR-8920239). This research was also supported by EAR-9304502 and EAR-9614612 grants to R.C.L. MPI contribution no. 224.

REFERENCES CITED

Bevington, P.R. and Robinson, D.K. (1996) Data reduction and error analysis for the physical sciences (2nd edition), p. 194–220. McGraw-Hill, New York.

Chai, M., Brown, J.M., and Slutsky, L.J. (1998) The elastic constants of Kilbourne Hole orthopyroxene to 12.5 GPa. Journal of Geophysical Research, 102, 14,779–14,785.

Cook, R.K. (1957) Variation of elastic constants and static strains with hydrostatic pressure: A method for calculation from ultrasonic measurements. Journal of the Acoustical Society of America, 29(4), 445–449.

Davies, G.F. and Dziewonski, A.M. (1975) Homogeneity and constitution of the Earth's lower mantle and outer core. Physics of the Earth and Planetary Interiors, 10, 336–343.

Davies, G.F. and O'Connell, R.J. (1977) Transducer and bond phase shifts in ultrasonics, and their effects on measured pressure derivatives of elastic moduli. In M. Manghnani and S. Akimoto, Eds., High Pressure Research: Application in Geophysics, p. 533–562. Academic Press, New York.

Flesch, L.M. (1997) Sound velocities of polycrystalline $MgSiO_3$-orthopyroxene to 10 GPa at room temperature. M.S. thesis, State University of New York at Stony Brook, Stony Brook, New York.

Frisillo, A.L. and Barsch, G.R. (1972) Measurement of single-crystal elastic constants of bronzite as a function of pressure and temperature. Journal of Geophysical Research, 77, 6360–6384.

Gasparik, T. (1990) Phase relations in the transition zone. Journal of Geophysical Research, 95, 15751–15769.

Gwanmesia, G.D. and Liebermann, R.C. (1992) Polycrystals of high-pressure phases of mantle minerals: Hot pressing and characterization of physical properties. In Y. Syono and M. Manghnani, Eds., High-Pressure Research: Application to Earth and Planetary Sciences, p. 117–135. American Geophysical Union, Washington, D.C.

Hugh-Jones, D.A. and Angel, R.J. (1994) A compressional study of $MgSiO_3$ orthoenstatite up to 8.5 GPa. American Mineralogist, 79, 405–410.

Hugh-Jones, D.A., Chopelas, A., and Angel, R.J. (1997) Tetrahedral compression in $(Mg,Fe)SiO_3$ orthopyroxenes. Physics and Chemistry of Minerals, 42, 301–310.

Ito, H., Mizutani, H., Ichinose, K., and Akimoto, S. (1977) Ultrasonic wave velocity measurements in solids under high pressure using solid pressure media. In M.H. Manghnani and S. Akimoto, Eds., High-Pressure Research: Applications in Geophysics, p. 603–622. Academic Press, New York.

Ito, J. (1975) High temperature solvent growth of orthoenstatite, $MgSiO_3$, in air. Geophysical Research Letters, 2, 533–535.

Jackson, I., Niesler, H., and Weidner, D.J. (1981) Explicit correction of ultrasonically determined elastic wave velocities for transducer-bond phase shift. Journal of Geophysical Research, 89, 3736–3748.

Knoche, R., Webb, S.L., and Rubie, D.C. (1995) Ultrasonic velocity to 10 GPa and 1500°C in the multi-anvil press: Measurements in polycrystalline olivine. Eos, 76, 563 p.

———(1996) In situ measurements of sound velocities at mantle conditions. Abstract from the US-Japan Seminar on High Pressure Research, Maui. American Geophysical Union, Washington, D.C.

Li, B., Jackson, I., Gasparik, T., and Liebermann, R.C. (1996a) Elastic wave velocity measurement in multi-anvil apparatus to 10 GPa using ultrasonic interferometry. Physics of the Earth and Planetary Interiors, 98, 79–91.

Li, B., Gwanmesia, G.D., and Liebermann, R.C. (1996b) Sound velocities of olivine and beta polymorphs of Mg_2SiO_4 at Earth's transition zone pressures. Geophysical Research Letters, 23, 2259–2262.

Li, B., Chen, G., Gwanmesia, G.D., and Liebermann, R.C. (1998) Sound velocity measurements at mantle transition zone conditions of pressure and temperature using ultrasonic interferometry in a multi-anvil apparatus. In M.H. Manghnani and Y. Syono, Eds., US-Japan Seminar on High Pressure Research. American Geophysical Union, Washington, D.C., (in press).

Niesler, H. and Jackson, I. (1989) Pressure derivatives of elastic wave velocities from ultrasonic interferometric measurements on jacketed polycrystals. Journal of Acoustical Society of America, 86, 1573–1585.

Pacalo, R.E.G. and Gasparik, T. (1990) Reversals of the orthoenstatite-clinoenstatite transition at high pressure and high temperatures. Journal of Geophysical Research, 95, 15853–15858.

Rigden, S.M., Gwanmesia, G.D., Jackson, I., and Liebermann, R.C. (1992) Progress in high-pressure ultrasonic interferometry. The pressure dependence of elasticity of Mg_2SiO_4 polymorphs and constraints on the composition of the transitions zone of the Earth's mantle. In Y. Syono and M. Manghnani, Eds., High Pressure Research; Application to Earth and Planetary Sciences, p. 167–182. American Geophysical Union, Washington D.C.

Sasaki, S., Takeuchi, Y., Fujuno, K., and Akimoto, S. (1982) Electron density distributions of three orthopyroxenes $Mg_2Si_2O_6$, $Co_2Si_2O_6$, and $Fe_2Si_2O_6$. Zeitschrift für Kristallograhpie, 156, 279–297.

Webb, S.L. and Jackson, I. (1990) Polyhedral rationalization of variation among the single-crystal elastic moduli for the upper-mantle silicates garnet, olivine, and orthopyroxene. American Mineralogist, 75, 731–738.

———(1993) The pressure dependence of the elastic moduli of single-crystal orthopyroxene $(Mg_{0.8},Fe_{0.2})SiO_3$. European Journal of Mineralogy, 5, 1111–1119.

Weidner, D.J., Wang, H., and Ito, J. (1978) Elasticity of orthoenstatite. Physics of the Earth and Planetary Interiors, 17, 7–13.

Zhao, Y., Schiferl, D., and Shankland, T.J. (1995) A high P-T single-crystal x-ray diffraction study of thermoelasticity of $MgSiO_3$ orthoenstatite. Physics and Chemistry of Minerals, 22, 393–389.

Manuscript received April 18, 1997
Manuscript accepted November 26, 1997
Paper handled by Robert W. Luth